SAND97-1230J

Solubility of Np(V) in K-Cl-CO_3 and Na-K-Cl-CO_3 Solutions to High Concentrations: Measurements and Thermodynamic Model Predictions

Ilham Al Mahamid, Craig F. Novak*, Kevin A. Becraft, Scott A. Carpenter, and Nadia Hakem

Lawrence Berkeley National Laboratory, Mail Stop 70A-1150, 1 Cyclotron Road, Berkeley, CA 94720 USA

* Sandia National Laboratories, P.O. Box 5800, Albuquerque, NM 87185-1320 USA

Abstract

Oversaturation experiments were performed to measure the Np(V) volubility in K-Cl-CO_3 and Na-K-Cl-CO_3 solutions to high concentrations. The resulting solution compositions and stable Np(V) solid phases were compared with predictions from a proposed thermodynamic data base for Np(V) volubility in concentrated Na-K-Cl-CO_3 electrolyte solutions (Novak et al., 1996a). Measurements in 3.2m KC1 plus 0.001, 0.01, or O. 1m K_2C0_3 eliminated a parameter redundancy in the data base. The resulting data base predictions match thirteen volubility measurements to within **0.5** logarithmic units, where the measurements were taken over wide concentration ranges in K-Cl-CO_3 media. In addition, results from six experiments in (5m NaCl + 0.1m KCl) with added Na_2C0_3 concentrations below 0.05m are predicted within **0.5** logarithmic units, while those with added Na_2C0_3 up to lm are predicted within 1.0 logarithmic unit. The thermodynamic data base also reproduces both the observed volubility-controlling solid phase and the total dissolved Np(V) concentrations in three complex synthetic brines with ionic strengths ranging from 0.8 to 7.8 molal. These comparisons demonstrate that solubility-limited aqueous Np(V) concentrations can be reliably predicted using the aqueous thermodynamics.

Introduction

A thermodynamic data base for describing the volubility of Np(V) in concentrated Na-K-Cl-CO_3 electrolytes has been proposed (Novak et al., 1996a). The data base is an extension of the Harvie et al. **(1984)** and Felmy and Weare (1986) thermodynamic data bases describing mineral solubilities in concentrated

groundwaters. Activity coefficients are calculated using the Pitzer activity coefficient formalism (Pitzer, 1991). The Np(V) parameters were based on measurements in which the dominant anionic bulk electrolyte was either Cl– or CO_3^{2-}, but not when both the chloride and carbonate ions were simultaneously present in large concentrations. The chemical systems used to parameterize the model resulted in a redundancy between the parameter describing K+ - $NpO_2(CO_3)_3^{5-}$ interactions and the parameter describing CO_3^{2-} - $NpO_2(CO_3)_3^{5-}$ interactions. To break this redundancy, additional measurements of the volubility of $KNpO_2CO_3(s)$ in K-C1-$C0_3$ media over large concentration ranges were required. Also, further experimental support was needed for the observation that the $KNpO_2CO_3(s)$ solid, not the $NaNp0_2C0_3 \cdot 3.5\,H_2O(s)$ solid, controls volubility even in solutions with large sodium concentrations (Novak et al., 1996b). Such experiments would provide independent chemical data to verify the thermodynamic data base developed for the Np(V)-Na-K-Cl-CO_3 system.

Experimental

All chemicals were A.R. grade, KOH from J.T. Baker and K_2C0_3 from Matheson, Coleman, and Bell. Filtration was performed with 4.1 nm Centricon filters from Amicon Corporation. X-ray capillaries were loaded into a Philips Debye-Scherrer 57.3 mrn camera, type 52056-B, using Kodak DEF392 films and copper K_α radiation filtered through a nickel filter. The equilibration vessels were made from polyetheretherketone (from Cadillac Plastics). All experiments were conducted under argon atmosphere at slightly elevated room temperature, 22±1°C.

Aqueous Np concentrations were measured using the 29.4 keV gamma ray. We used a high purity germanium (HPGe) detector of Lawrence Berkeley National Laboratory design with a full width half-maximum (FWHM) resolution of about 0.5keV. The overlap from the ^{233}Pa gamma ray peak at 28.6 keV was removed by applying spectral deconvolution. The correction was only necessary in the samples at very low Np concentrations ($<10^{-6}$ M).

Experiment Preparation

Two series of experiments were conducted, one in $K\text{-}Cl\text{-}CO_3$ solutions and one in $Na\text{-}K\text{-}Cl\text{-}CO_3$ solutions. Thirteen reaction vessels were prepared for the $K\text{-}Cl\text{-}C0_3$ series with K_2C0_3 concentrations ranging from 0.001 to 1.0m and KC1 concentrations ranging from 0.0032 to 3.2m. The $K\text{-}Cl\text{-}CO_3$ solution compositions are reported Table 1. Undersaturation experiments were started by adding freshly precipitated $KNp0_2C0_3(s)$ (or $NpO_2OH(am)$ in one reaction vessel) prepared as described previously (Novak et al., 1996a). Eight reaction vessels were prepared for the $Na\text{-}K\text{-}Cl\text{-}CO_3$ series with Na_2C0_3 concentrations ranging from 0.00032 to 1m in solutions of 5m NaCl + O. 1m KC1. The $Na\text{-}K\text{-}Cl\text{-}CO_3$ solution compositions are reported in Table 2. Undersaturation experiments were started with $KNpO_2CO_3(s)$ for carbonate concentrations less than or equal to 0.01m and with $Na_3Np0_2(C0_3)_2(s)$ for carbonate concentrations greater than or equal to 0.01m. Note that two vessels were started at 0.01m Na_2C0_3, one with each solid. These initial solid phases were chosen based *on* preliminary thermodynamic modeling of volubility data for Np(V) in K_2C0_3 media (Novak et al., 1996a).

$Na_3Np0_2(C0_3)_2(s)$ was prepared by adding 1M Na_2C0_3 to the Np(V) stock solution to obtain a final carbonate concentration of about 0.5M. A white precipitate was formed. A duplicate precipitate was prepared for x-ray analysis to verify the structure of this initial solid used to start the experiments.

For routine analysis, a sample from each vessel was collected, filtered, and analyzed for Np concentration. The pH was measured using a Ross combination glass electrode that had been calibrated in each of the corresponding K-Cl and Na-K-Cl solutions to account for liquid junction potential. The total inorganic carbon (TIC) content was also monitored to detect any large changes in solid TIC, but because these solutions generally had large carbonate concentrations, were highly basic, and were in tightly sealed vessels under argon, no significant loss or gain of TIC was noted.

Results

The $K\text{-}Cl\text{-}CO_3$ series of experiments was allowed to react for 168 days, with steady state being achieved within 108 days of reaction time; see Figure 1. At carbonate concentrations less than 0.0 lm, dissolved Np(V) concentrations decrease as the KCl concentration increases, reflecting the dominant equilibrium

$$KNpO_2CO_3(s) \leftrightarrow K^+ + NpO_2CO_3^- \quad (1)$$

At carbonate concentrations greater than 0.0 lm, Np(V) dissolved concentrations increase as the KC1 concentration increases, which is counter to the dominant equilibrium

$$KNpO_2CO_3(s) + 2\ CO_3^{2-} \leftrightarrow K^+ + NpO_2(CO_3)_3^{5-} \quad (2)$$

Here, the large potassium ion concentrations and large ionic strengths stabilize the highly negatively-charged neptunyltriscarbonato ion, which results in the opposite trend than would be obtained by simply applying Le Chatlier's Principle.

X-ray powder diffraction analysis of the final solid phases in the $K\text{-}Cl\text{-}CO_3$ series produced patterns identical to those of the initial solid $KNpO_2CO_3(s)$ in all but the most concentrated solution. With concentrations $m_{KCl}=1.0$ and $m_{K_2CO_3}=1.0$, both $KNpO_2CO_3(s)$ and $NpO_2OH(am)$ were converted to $K_3Np0_2(C0_3)_2(s)$. The powder pattern for these final solids are the same as those reported in Novak et al. (1996a). Several representative patterns are given in Table 3.

The $Na\text{-}K\text{-}Cl\text{-}CO_3$ series of experiments was allowed to react for 170 days. Comparison of the measurements for day 107 and day 170 suggest that these experiments were at steady state conditions; see Figure 2.

X-ray powder diffraction analyses for the $Na\text{-}K\text{-}Cl\text{-}CO_3$ series, reported in Table 4, indicate that the solid phases remained unchanged for all but the most concentrated solution. That is, $KNpO_2CO_3(s)$ remained present in solutions with

carbonate concentrations less than 0.01m, and $Na_3NpO_2(CO_3)_2(s)$ remained in solutions with carbonate concentrations between 0.01 and 0.2m. Both solids remained in the 0.01m carbonate solution suggesting that either that one of the solids is metastable or that the solution composition is such that both are approximately identically saturated. The X-ray powder diffraction pattern for the solid from the $m_{Na^+}=7, m_{K^+}=0.1, m_{Cl^-}=5, m_{CO_3^{2-}}=1$, given in Table 4, does not match any of the patterns for sodium or potassium neptunyl(V) solids found in the literature.

Comparison with Thermodynamic Model

Thermodynamic calculations were performed using the FMT volubility and speciation computer code (Babb and Novak, 1995) using the thermodynamic parameters for concentrated electrolyte solutions from Harvie et al. (1984) and Felmy and Weare (1986). Code version and file information is given under Acknowledgements. All Np(V) parameters were taken from Novak et al. (1996a) and references therein.

K-Cl-CO_3 Solutions

A recently proposed set of thermodynamic parameters for Np(V) in Na-K-Cl-CO_3 media (Novak et al., 1996a) contained a redundancy in ion interaction parameters expressed by the relationship $2\beta^{(0)}_{KX} + \theta_{CO_3X} = 2.80$, where $X = NpO_2(CO_3)_3^{5-}$. These parameters were shown to describe Np(V) volubility data in K_2CO_3 media equally well for $-1.9 \le \theta_{CO_3X} \le 0$. The experiments in K-Cl-CO_3 media with high carbonate and high chloride concentration can be used to break this redundancy because the neptunyl tricarbonato ion is the dominant Np(V) species and thus CO_3^{2-} interactions with $NpO_2(CO_3)_3^{5-}$ are significant. A comparison of the results from the K-Cl-CO_3 experiments with $m_{KCl}=3.2$ and model calculations with $\theta_{CO_3X}=0$, –0.83, and –1.9 ($\beta^{(0)}=1.41, 1.82$, and 2.35, respectively) is given in Figure 3. As can be seen, the parameter sets with $\theta_{CO_3X}=0$ and $\theta_{CO_3X}=-0.83$ significantly overpredict the volubility of $KNpO_2CO_3(s)$ under these conditions by more than one

and two orders of magnitude, respectively. The parameter set with ε_{CO_3X}=–1.9 provides excellent agreement with these data, leading us to select this parameter set as the best. In these solutions, the larger value of $\beta^{(0)}$ increases the activity coefficient of $NpO_2(CO_3)_3^{5-}$ and thus suppresses the solution concentration of $NpO_2(CO_3)_3^{5-}$, and this effect dominates over the decrease in activity coefficient caused by CO_3-$NpO_2(CO_3)_3^{5-}$ interactions. A similar though less pronounced trend occurs in the m_{KCl}=0.32 solutions, but the difference is less than 0.25 log units at $0.1m_{CO_3^{2-}}$.

The volubility data and speciation calculations as a function of K_2C0_3 are summarized for the 0.0032, 0.032, 0.32, and 3.2m KC1 solutions in Figures 4a-d. The speciation curves in the 0.0032, 0.032, and 0.32 m KC1 are plotted up to approximately the concentration where $K_3NpO_2(CO_3)_2$(s) becomes the thermodynamically predicted stable phase. The precipitation of $K_3NpO_2(CO_3)_2$(s) was suppressed in the predictions for 3.2m KC1 to facilitate comparison with the solid phases observed in the experiments. The bold vertical line indicates the approximate concentrations where $K_3NpO_2(CO_3)_2$(s) would become the more stable phase. Thus, the data point at $m_{K_2CO_3}$=0.1 and m_{KCl}=3.2 represents a metastable equilibrium of $KNpO_2CO_3$(s).

All of the data in Figures 4a-d test the volubility product value for $KNpO_2CO_3$(s). At the lower concentrations, the data test the thermodynamic parameters for the $NpO_2CO_3^-$ species. At the higher concentrations, the data test the parameters for the $NpO_2(CO_3)_3^{5-}$ species. The $NpO_2(CO_3)_2^{3-}$ species is predicted to be dominant only under narrow ranges of the conditions studied here, and these ranges were not sufficiently examined in this experimental work to draw comparisons with the data base predictions. The calculations agree with the data within 0.3 log units at low concentrations and within 0.1 log units at high concentrations, reflecting the predominance of high concentration data for determining model parameters. The agreement at low concentrations suggest that

the assignment of Na^+-$NpO_2CO_3^-$ parameters to K^+-$NpO_2CO_3^-$ parameters is justified (Novak et al., 1996a).

Only for the solutions with $m_{K_2CO_3}=m_{KCl}=1$ was the $K_3Np0_2(C0_3)_2(s)$ phase observed. The separate reaction vessels, started with either $Np0_20H(am)$ or $KNpO_2CO_3(s)$, yielded total Np aqueous concentrations of $10^{-4.71}$ and $10^{-4.74}$ molal, respectively. The data base predictes that the volubility of $K_3Np0_2(C0_3)_2(s)$ yields a total Np(V) concentration of $10^{-4.75}$m under these conditions. Although additional data are required to test the utility of the data base for calculating the volubility of this potassium neptunyl carbonato solid, the reproducibility of the data and the agreement between the predictions and data suggest that the volubility product value is reliable.

In summary, the thermodynamic parameters of Novak et al. (1996a) provide excellent predictions of all Np(V) volubility measurements made over wide ranges of K-Cl-CO_3 solution compositions.

Na-K-Cl-CO_3 Solutions

A comparison of the data in Na-K-Cl-CO_3 solutions and the predicted volubility and speciation from the thermodynamic data base is given in Figure 5. The $KNpO_2CO_3(s)$ solid is predicted to be stable below about 0.006m total carbonate concentration under these conditions, in agreement with the experimental observations. The predicted total Np(V) concentrations are within 0.5 log units. The model indicates that $KNpO_2CO_3(s)$ is not the most stable solid phase at 0.01m carbonate ion, but the predictions of $KNpO_2CO_3(s)$ volubility under these conditions agrees well with the measured value. The lack of conversion from the monopotassium to the trissodium solid under these conditions may reflect a kinetic barrier to solid phase conversion that would be consistent with that observed between the monopotassium and trispotasium neptunyl carbonato solids (Novak et al., 1996a).

The $Na_3Np0_2(C0_3)_2(s)$ solid is predicted to be stable above about 0.006m total carbonate concentrations under these conditions. The predictions agree well with measurements for 0.01 and 0.045m carbonate ion, but deviate in the higher concentration solutions by up to 0.8 log units. Little can be concluded from the comparison between the model and the data point in the most concentrated solutions because the solid has not been identified.

These experiments provide an additional test of the volubility product for $KNpO_2CO_3(s)$ and $Na_3Np0_2(C0_3)_2(s)$, and demonstrate that the potassium solid forms even when the sodium concentration is fifty times greater. Note that these experiments primarily test the ion interaction parameter values between the neptunyl carbonato species and the sodium ion, not with the potassium ion, because the sodium concentration is so much larger. The good agreement between predictions and experiment below O. lm carbonate indicate that these parameters are reliable. The deviation between predictions and experiment at higher carbonate concentrations suggests that the ion interaction parameter values between the sodium and neptunyl triscarbonato ion could be improved, perhaps with the addition of a C^{ϕ}_{NaX} parameter. However, it must be recognized that these highly concentrated solutions represent an extrapolation of the Fanghänel et al. (1995) data base beyond the sodium concentrations used to fit the ion interaction parameters.

In summary, the thermodynamic parameters of Novak et al. (1996a) provide excellent predictions of the Np(V) volubility measurements made in concentrated $Na\text{-}K\text{-}Cl\text{-}CO_3$ solutions when the carbonate concentration is less than about 0.1 molal, which includes most environmentally relevant conditions.

Model Comparison with Data from Complex Synthetic Brines

The thermodynamic model and data base of Novak et al. (1996a) can also be tested through comparisons with volubility measurements in complex synthetic brines. Two such experiments were performed in predominantly Na-Cl brines

containing small amounts of Mg, Ca, and K. Another such experiment was performed in a predominantly Na-Mg-K-Cl brine. These experiments, in which $CO_2(g)$ partial pressures and the pH meter reading were held constant, are reported in Novak et al. (1996b). The solution compositions are given in Table 5.

The operational pH measurements were taken with Ross electrodes calibrated to standard low ionic strength buffer solutions (Novak et al., 1996 b), but calibrations to determine the correction for liquid junction potentials were not performed. To develop the correspondence between meter reading and the hydrogen ion concentration, the operational pH values, pH_{op}, were converted to hydrogen ion modalities using the electrode calibration equation

$$pmH \equiv -\log m_{H^+} = pH_{op} + 0.159\, m_{NaCl} + \log\left(\frac{m}{M}\right) \qquad (3)$$

reported by Rai et al. (1995), where $\frac{m}{M}$ is the ratio of molality to molarity, given in Table 5.

The meter readings pH_{op} = 7.5±0.1 and 7.1±0.1 for the two predominantly NaCl brines were converted to $pmH=-\log(m_{H^+})$ = 7.6±0.25 and 7.6±0.25 using the ionic strength of the solutions to approximate m_{NaCl}. Because of the uncertainty associated with this estimation, the error was arbitrarily increased from ±0.1 to ±0.25 units to reflect the lack of precise knowledge of the pmH. The meter reading for the Na-Mg-K-Cl brine, pH_{op}=7.3±0.1 was converted to pmH=8.6±0.5, again using the ionic strength to approximate m_{NaCl}. However, because this brine is very different from NaCl, having $m_{Mg^{2+}}$=1.6 and m_{K^+}=0.8, we have arbitrarily increased the uncertainty from ±0.1 to ±0.5 units. The minimum and maximum dissolved Np(V) concentrations given below correspond to the highest and lowest concentrations predicted over the pmH ranges given above.

For the purposes of the simulations below, several carbonate solids in the Harvie et al. (1984) data base were prevented from precipitating, including aragonite and calcite, both $CaCO_3(s)$, dolomite, $CaMg(CO_3)_2(s)$, gaylussite, $CaNa_2(CO_3)_2 \cdot 5H_2O(s)$, magnesite, $MgCO_3(s)$, magnesium oxychloride,

$Mg_2Cl(OH)_3 \cdot 4H_2O$(s), nesquehonite, $MgCO_3$ ● 3HQO(S), and pirssonite, $Na_2Ca(CO_3)_2 \cdot 2H_2O$ (s). None of the characteristic X-ray diffraction patterns for these solids were identified in the experiments reported in Novak et al. (1996b).

The volubility of Np(V) in the 0.86 and 3.0 molal brines was reported to be $(1.94\pm0.58)\times10^{-6}$ M and $(8.2\pm3.9)\times10^{-7}$ M (Novak et al., 1996 b), or $\log(m_{Np(V)})= -5.73\pm0.13$ and -6.12 ± 0.22, respectively. The solid phases isolated from the brine experiments were identified as $KNpO_2CO_3$(s). The thermodynamic parameter set from Novak et al. (1996a) predicts total dissolved Np(V) COnCentratiOnS Of $\log(m_{Np(V)})= -5.1$ to -5.8 for the 0.86m brine, and $\log(m_{Np(V)})= -5.3$ to -6.0 in the 3.0m brine. The predicted volubility and speciation of Np(V) in these brines are given in Figures 6a and 6b, respectively. $KNpO_2CO_3$(s) is predicted to be the most stable solid phase, that is, all other Np(V) solids in the data base are under saturated, including $Np0_20H$(aged), $NaNp0_2C0_3^0 3.5H_20$ (s), $Na_3Np0_2(C0_3)_2$(s), and $K_3NpO_2(CO_3)_2$(s). The curves are plotted up to around pmH=9, where $Na_3NpO_2(CO_3)_2$(s) becomes the predicted stable solid phase. The thermodynamic model thus predicts both the correct solid phase and the total Np(V) concentrations within the uncertainty associated with the calculations and measurements.

The volubility of Np(V) in the 7.8 molal ionic strength brine was reported to be $(2.38\pm0.80)\times10^{-7}$ M (Novak et al., 1996b), or $\log(m_{Np(V)})= -6.60\pm0.15$, and the solid phase was identified as $KNpO_2CO_3$(s) as well. Direct Np(V) volubility predictions in this brine using the data base of Novak et al. (1996a) yield the observed solid, $KNpO_2CO_3$(s), but give a volubility 4 to 5 orders Of magnitude higher than that measured. This difference is probably because the thermodynamic data base does not include ion interaction parameters between Mg^{2+} and the neptunyl carbonato anions. 'We can approximate the ion interaction parameters for Mg^{2+} and the neptunyl carbonato ions as the average of the parameter values for Na^+ and K^+, that is, $\beta^{(0)}_{MgNpO_2CO_3}$ ·10, $\beta^{(1)}_{MgNpO_2CO_3}$ · 34, $\beta^{(0)}_{MgNpO_2(CO_3)_2}=0.48$, $\beta^{(1)}_{MgNpO_2(CO_3)_2}=4.4$, $\beta^{(0)}_{MgX}=2.07$, $\beta^{(1)}_{MgX}=22.7$, $\beta^{(2)}_{MgX}=-48$, and $C^{\phi}_{MgX}=-0.11$. This is a

reasonable first approximation, although no attempt was made to correlate between monovalent and divalent ions. Using these assignments, the data base predictions provide a remarkably good estimate of the volubility, as shown in Figure 6c. The curves stop around pmH=9 because of the incipient precipitation of brucite, $Mg(OH)_2(s)$, which has been observed to form in the laboratory under these conditions. The assignment of parameter values for interactions between Mg^{2+} and the neptunyl carbonato anions effectively suppressed the formation of the neptunyl his- and triscarbonato ions in this brine while having almost no effect on the neptunyl monocarbonato ion concentration. Obviously, more data in solutions with high magnesium content are necessary to support and confirm the thermodynamic data base under these conditions.

The thermodynamic predictions for Np(V) volubility in the three synthetic brines are very satisfactory, agreeing with measured values to within less than an order of magnitude. These results demonstrate that reliable prediction of dissolved Np(V) concentrations in complex concentrated electrolyte solutions under environmentally relevant conditions is possible. In addition, this work demonstrates that combination of thermodynamic parameters determined in simpler media, in this case Np(V) in $NaClO_4$, NaCl, $NaClO_4$ with $CO_2(g)$, NaCl with $CO_2(g)$, Na_2CO_3, and K_2CO_3, can produce a reliable and robust data base for predicting solubilities in complex ionic media.

Critical Assessment of Overall Np(V) Solubility Data Base

The thermodynamic model and data base calculates the importance of competing chemical effects that stabilize or destabilize the neptunyl triscarbonato ion. The parameter set that provides the best comparison with these data, $\beta^{(0)}_{NaX}$=1.80, $\beta^{(0)}_{KX}$=2.35, θ_{ClX}=–0.26, θ_{CO_3X}=–1.9, where X= $NpO_2(CO_3)_3^{5-}$, indicates that an increase in Na^+ or K+ concentration will lower the solution concentration of $NpO_2(CO_3)_3^{5-}$ by increasing y_x, while an increase in the Cl– or CO_3^{2-} concentration will raise the solution concentration of $NpO_2(CO_3)_3^{5-}$ by decreasing Y_x. The magnitude and signs of the parameters in this set, while providing an excellent

description of a wide range of data (Fanghänel et al., 1995; Novak et al., 1996a; this work), do not necessarily make a great deal of chemical sense.

This state of affairs is due in large part to the choice of the perchlorate ion as a reference state, i. e., the assignment of $\theta_{NpO_2ClO_4} = \theta_{NpO_2(CO_3)_2ClO_4} = \theta_{NpO_2(CO_3)_3ClO_4} = 0$ (Fanghänel et al., 1995). Consider the series $\theta_{ClO_4X} = 0, \theta_{ClX} = -0.26, \theta_{CO_3X} = -1.9$, which suggests that the ClO_4^- ion has the largest influence of the three anions in destabilizing the neptunyl triscarbonato ion in solution. Examining the parameter set with the benefit of the entire suite of data now available illustrates the influence of the reference state on the magnitude of parameters based upon the reference value. In this light, it seems that positive values for θ_{ClO_4X} and θ_{ClX} would better represent the observation that the presence of the perchlorate and chloride anions destabilize the neptunyl triscarbonato ion. The value for θ_{CO_3X} would remain negative, reflecting a stabilization effect of carbonate ions on the neptunyl triscarbonato ion, perhaps through promotion of ligand exchange. The entire volubility model would need to be parameterized to realize this change. This would most probably decrease the magnitude of the $\beta^{(0)}$ parameters to result in less suppression of the neptunyl triscarbonato species, relative to the Debye-Hückel term. The resulting reparameterized model would not describe the existing data any better than the current one, but the significance of each of the parameters would be more intuitive chemically, and the magnitude of the parameters would be more in agreement with other parameters reported in the literature.

Acknowledgments

This work was supported by the United Stated Department of Energy under Contract DE-AC04-94AL85000. Sandia is a multiprogram laboratory operated by Sandia Corporation, a Lockheed Martin Company, for the United States Department of Energy.

This work was performed as part of the Waste Isolation Pilot Plant (WIPP) Actinide Source Term Program. Laboratory work was performed at the Lawrence Berkeley National Laboratory under contract M-I-5592 with SNL, under a Sandia-approved Quality Assurance program.

All equilibrium calculations were made using FMT v2.2 resident under SCMS on the WIPP Alpha computers as file FMT_FMT2PO_PA96_2 .EXE. The files used and generated are:

Solubility System	Data Base (. CHEMDAT file)	File Identifier
3.2m KCl as a function of K2C03 (Figure 3) with θ=-1.9	FMT_960823NONP312	FMT_NP_KCLC03_3P0
as above, except with 8=-0.83	replace the appropriate -1.9 with -0.83 and rerun	FMT_NP_KCLC03_3P0
as above, except with θ=0.0	replace the appropriate -1.9 with -0.83 and rerun	FMT_NP_KCLC03_3P0
0.0032m KCl as a function of K2C03 (Figure 4a)	FMT_HMW_AM3PU3TH4NP5_960823	FMT_NP_KCLC03_0P003
0.032m KCl as a function of K2C03 (Figure 4b)	FMT_HMW_AM3PU3TH4NP5_960823	FMT_NP_KCLC03_0P03
0.32m KC1 as a function of K2C03 (Figure 4c)	FMT_HMW_AM3PU3TH4NP5_960823	FMT_NP_KCLC03_0P3
3.2m KC1 as a function of K2C03 (Figure 4d)	FllT_960823NONP312	FMT_NP_KCLC03_3P0
5.0m NaCl plus 0.1m KC1 as a function of Na2C03 (Figure 5)	FMT_HMW_AM3PU3TH4NP5_960823	FMT_NP_NAKCLC03
Metastable KNp02C03(s) in 5.0m NaCl plus 0.1m KC1 as a function of Na2C03 (Figure 5)	FflT-960823NONP312	FMT_NP_NAKCLC03_K 111
WIPP AISinR Brine (Figure 6a)	FMT_960823_AIS	FMT_NP_AIS
WIPP H17 Brine (Figure 6b)	FMT_960823_H17	FMT_NP_H17
UIPP SPC Brine (Figure 6c)	FMT_960823_SPC	FMT_NP_SPC
1mK2C03 plus 1mKCl (discussed in the prose)	FMT_HMW_AM3PU3TH4NP5_960823	FMT_NP_1MK2C03_1MKCL

All runs require .COM, .IN, and .INGUESS files. All runs produce a .TITRATE file as the pertinent output except the last, which produces a .OUT file as therelavent output file.

References

Babb, S. C., and C.F. Novak. 1995. "FMT, Version 2.00, User's Manual." Albuquerque, New Mexico: Sandia National Laboratories. SWCF WPO 28119.

Fanghänel, Th., V. Neck, and J.I. Kim. 1995. "Thermodynamics of Neptunium(V) in Concentrated Salt Solutions: II. Ion Interaction (Pitzer) Parameters for Np(V) Hydrolysis Species and Carbonate Complexes." *Radiochimica Acts* vol. **69: 169-173.**

Felmy, A. R., and J.H. Weare. 1986. "The Prediction of Borate Mineral Equilibria in Natural Waters: Application to Searles Lake, California. " *Geochimica et Cosmochimica Acts* vol. *50: 2771-2783.*

Harvie, C. E., N. Møller, and J.H. Weare. 1984. "The Prediction of Mineral Solubilities in Natural Waters: The Na-K-Mg-Ca-H-Cl-SO_4-OH-HCO_3-CO_3-CO_2-H_2O System to High Ionic Strengths at 25°C." *Geochimica et Cosmochimica Acts* vol. **48: 723-751.**

Novak, C. F., I. Al Mahamid, K.A. Becraft, S.A. Carpenter, N. Hakem, and T. Prussin. 1996a. "Measurement and Thermodynamic Modeling of Np(V) Volubility in Dilute Through Concentrated K_2C0_3 Media." SAND96-1604J. Albuquerque, New Mexico: Sandia National Laboratories.

Novak, C. F., H. Nitsche, H.B. Silber, K. Roberts, Ph.C. Torretto, T. Prussin, K. Becraft, S.A. Carpenter, D.E. Hobart, and I. Al Mahamid. 1996b. "Neptunium(V) and Neptunium(VI) Solubilities in Synthetic Brines of Interest to the Waste Isolation Pilot Plant (WIPP)." *Radiochimica Acts* vol. **74: 31-36.**

Pitzer, K.S. 1991. "Ion Interaction Approach: Theory and Data Correlation." Chapter 3, pp. 75-153 in *Activity Coefficients in Electrolyte Solutions.* K.S. Pitzer, editor. Boca Raton, Florida: CRC Press.

Rai, D., A.R. Felmy, S.P. Juracich, and L. Rae. 1995. *Estimating the Hydrogen Ion Concentration in Concentrated NaCl and Na_2SO_4 Electrolytes. SAND94-1949.* Albuquerque, New Mexico: Sandia National Laboratories. (Note that because of a typographical error, the printed report incorrectly lists Rae's first name as Finfeng when it is Linfeng.)

Table 1. Solution compositions and measured Np(V) concentrations for the K-Cl-CO_3 series of experiments.

KCl (m)	K_2CO_3 (m)	Np [M]	starting solid
0.0034	0.0010	$(1.21 \pm 0.08)\times10^{-6}$	$KNpO_2CO_3(s)$
0.0032	0.0101	$(6.61 \pm 0.57)\times10^{-7}$	$KNpO_2CO_3(s)$
0.0323	**0.0010**	**(5.89 ± 0.28)x1 o-7**	$KNpO_2CO_3(s)$
0.0320	0.0101	(3.47 ± 0.24)x1 0^{-7}	$KNpO_2CO_3(s)$
0.0321	0.1001	(2.50 ± 0.32)x10+	$KNpO_2CO_3(s)$
0.3201	**0.0010**	**(2.32** $\pm 0.24)\times10^{-7}$	$KNpO_2CO_3(s)$
0.3200	**0.0101**	**(3.92** $\pm 0.38)\times$ **I o-7**	$KNpO_2CO_3(s)$
0.3200	0.1001	$(3.71 \pm 0.25)\times10^{-6}$	$KNpO_2CO_3(s)$
3.2000	0.0010	(1.94 ± O.24)X1O-7	$KNpO_2CO_3(s)$
3.1997	0.0101	(2.24 ± 0.32)x1 o-7	$KNpO_2CO_3(s)$
3.1997	0.1000	$(1.46 \pm 0.12)\times10^{-5}$	$KNpO_2CO_3(s)$
1.000	**0.996**	$(1.68 \pm 0.10)\times10^{-5}$	$KNpO_2CO_3(s)$
1.078	**1.072**	**(1.82 *0.12)X1 O-5**	$NpO_2OH(am)$

Table 1. Solution compositions and measured Np(V) concentrations for the K-Cl-CO_3 series of experiments.

KCl (m)	K_2CO_3 (m)	Np [M]	starting solid
0.0034	0,0010	$(1.21 \pm 0.08) \times 10^{-6}$	$KNpO_2CO_3(s)$
0.0032	0.0101	(6.61± 0.57) X50-7	$KNpO_2CO_3(s)$
0,0323	0.0010	(5.89 ± 0.28) x10_7	$KNpO_2CO_3(s)$
0.0320	0.0101	(3.47 ± 0.24)x1@	$KNpO_2CO_3(s)$
0.0321	0.100	$(2.50 \pm 0.32) \times 10^{-6}$	$KNpO_2CO_3(s)$
0.320	0.0010	$(2.32 \pm 0.24) \times 10^{-7}$	$KNpO_2CO_3(s)$
0.320	0.0101	$(3.92 \pm 0.38) \times 10^{-7}$	$KNpO_2CO_3(s)$
0,320	0.100	$(3.71 \pm 0.25) \times 10^{-6}$	$KNpO_2CO_3(s)$
3.20	**0.0010**	$(1.94 \pm 0.24) \times 10^{-7}$	$KNpO_2CO_3(s)$
3.20	**0.0101**	$(2.24 \pm 0.32) \times 10^{-7}$	$KNpO_2CO_3(s)$
3.20	**0.100**	$(1.46 \pm 0.12) \times 10^{-5}$	$KNpO_2CO_3(s)$
1.00	**0.996**	$(1.68 \pm 0.10) \times 10^{-5}$	$KNpO_2CO_3(s)$
1.08	**1.07**	$(1.82 \pm 0.12) \times 10^{-5}$	$NpO_2OH(am)$

Table 2. Solution compositions and measured Np(V) concentrations for the Na-K-Cl-CO_3 series of experiments.

NaCl (m)	KCl (m)	Na_2CO_3 (m)	Np (M)	starting solid
5.00	0.100	0.00035	$(1.04\pm0.41)\times10^{-6}$	$KNpO_2CO_3(s)$
5.00	0,100	0.00100	$(1.1\ 5\pm0.42)\times10^{-6}$	$KNpO_2CO_3(s)$
5.00	0.100	0.00310	$(2.11\pm0.99)\times10^{-6}$	$KNpO_2CO_3(s)$
5.00	0.100	0.00995	$(1.40\pm0.45)\times10^{-5}$	$KNpO_2CO_3(s)$
5.00	0.100	0.00995	$(6.32\pm0.23)\times10^{-5}$	$Na_3NpO_2(CO_3)_2(s)$
5.00	0.100	0.0454	$(3.55\pm0.13)\times10^{-4}$	$Na_3NpO_2(CO_3)_2(s)$
5.00	0.100	0.215	(4. O91O.13)X1F	$Na_3NpO_2(CO_3)_2(s)$
5.00	0.100	1.00	@#47to.11)$\times10^{-4}$	$Na_3NpO_2(CO_3)_2(s)$

Table 4. X-ray diffraction patterns for $KNpO_2CO_3(s)$, $Na_3NpO_2(CO_3)_2(s)$, and an unidentified solid from cells containing 5.0 m NaCl, 0.1 m KCl, and various concentrations of Na_2CO_3. Relative intensities on a scale from 1 to 10 are given in parentheses.

0.001 m Na_2CO_3	0.003 m Na_2CO_3	0.01 m Na_2CO_3	0.01 m Na_2CO_3	0.05 m Na_2CO_3	0.2 m Na_2CO_3	1.0 m Na_2CO_3
$KNpO_2CO_3(s)$	$KNpO_2CO_3(s)$	$KNpO_2CO_3(s)$	$Na_3NpO_2(CO_3)_2(s)$	$Na_3NpO_2(CO_3)_2(s)$	$Na_3NpO_2(CO_3)_2(s)$	unidentified
5.13 (3)		5.09 (3)	9.75 (1)	9.95 (1)		
4.40 (2)			8.47 (1)	8.46 (2)		
4.03 (lo)	4.07 (4)	4.03 (9)				7.39 (1)
3.33 (4)	3.35 (1)	3.36 (4)		6.92 (3)	6.85 (2)	
2.70 (1)	2.69 (1)					6.24 (1)
2.55 (9)	2.55 (3)	2.55 (6)	6.06 (3)	6.07 (4)		
			5.82 (3)	5.83 (4)		
2.28 (2)		2.29 (2)				5.24 (1)
				4.87 (2)	4.87 (1)	
2.16 (7)	2.16 (3)	2.16 (4)	4.39 (1 o)	4.40 (lo)	4.39 (lo)	
2.02 (1)			4.26 (2)	4.25 (2)		
1.99 (5)	1.99 (lo)	1.99 (lo)				4.14 (6)
			4.02 (6)	4.03 (7)	4.00 (7)	
1.85 (1)	1.86 (2)	1.85 (2)		3.66 (2)	3.62 (1)	3.34 (2)
1.80 (1)	1.81 (1)	1.80 (2)	3.21 (1)	3.22 (2)	3.21 (2)	
	1.76 (2)	1.74 (4)	3.10(1)			
1.64 (2)	1.65 (1)	1.64 (3)	2.99 (2)	3.00 (3)		3.03 (3)
1.58 (1)			2.93 (2)	2.93 (3)		
1.50 (2)		1.50 (3)	2.80 (1)	2.81 (1)		2.82 (2)
			2.54 (7)	2.54 (9)	2.54 (8)	2.54 (2)
			2.32 (1)			
						2.27 (2)
	1.24 (2)		2.19 (5)	2.20 (6)	2.20 (6)	
	1.21 (1)		2.12(1)	2.13 (1)		
				2.03 (2)		
				1.99 (5)	1.99 (9)	1.99 (lo)
				1.95 (1)		
				1.92 (1)		
			1.78 (7)			
						1.73 (3)
			1.70 (3)			
				1.66 (2)	1.66 (3)	
				1.47 (2)	1.47 (3)	
				1.26 (3)		1.24 (2)

Table 5. Summary of solution compositions and volubility predictions for $KNpO_2CO_3(s)$ in synthetic predominantly Na-Cl and Na-Mg-K-Cl brines. The composition of AISinR and H17 Brines are based on measurements of WIPP brines in the CUlebra Member of the Rustler Formation at the Air Intake Shaft and hydropad H-17, respectively. The composition of SPC Brine is based on the "Brine A" composition intended to represent brines from the WIPP repository horizon.

	AISinR Brine		H17 Brine		SPC Brine	
	molal	(Molar)	molal	(Molar)	molal	(Molar)
Na	0.656	(0.646)	2.54	(2.40)	2.06	(1.84)
K	3.00828	(0.0081 6)	).0324	(0.0307)	0.859	(0.766)
Mg	3.0218	(0.0215)	).0784	(0.0741)	1.61	(1 .43)
Ca	0.0174	(0.0171)	).0306	(0.0289)	0.0167	(0.0149)
cl	3.577	(0.568)	2.63	(2.48)	6.05	(5.39)
S (as SO_4)	0.0808	(0.0796)	3.0794	(0.0750)	0.0489	(0.0436)
B	3.00283	(0.00279	3.00421	(0.00398)	0.0229	(0.0204)
Br	0	(o)	3.00100	(0.000950)	0.00566	(0.00504)
Np(V)	$10^{-5.60}$	(1 0-5.61)	$10^{-5.80}$	(1 0-5.83)	10-6.58	(1 0-6.62)
Total Inorganic Carbon"	0.00347	(0.00342)	2.00274	(0.00260)	0.00152	(0.00135)
$P_{CO2(g)}$	$10^{-2.71}$		$10^{-2.56}$		1 ()-3.95	
estimated density, g/cm^3	1.03		1.10		1.20	
$\frac{m}{M}$	1.01		1.06		1.12	
Ionic Strength (molal)	0.862		2.98		7.82	
pmH J $-\log(m_{H+})$	7.67		7.65		8.56	
Total Dissolved Solids, mg/L	44,600		155,000		305,000	

• Total Inorganic Carbon concentration was calculated from the $CO_2(g)$ fugacity.

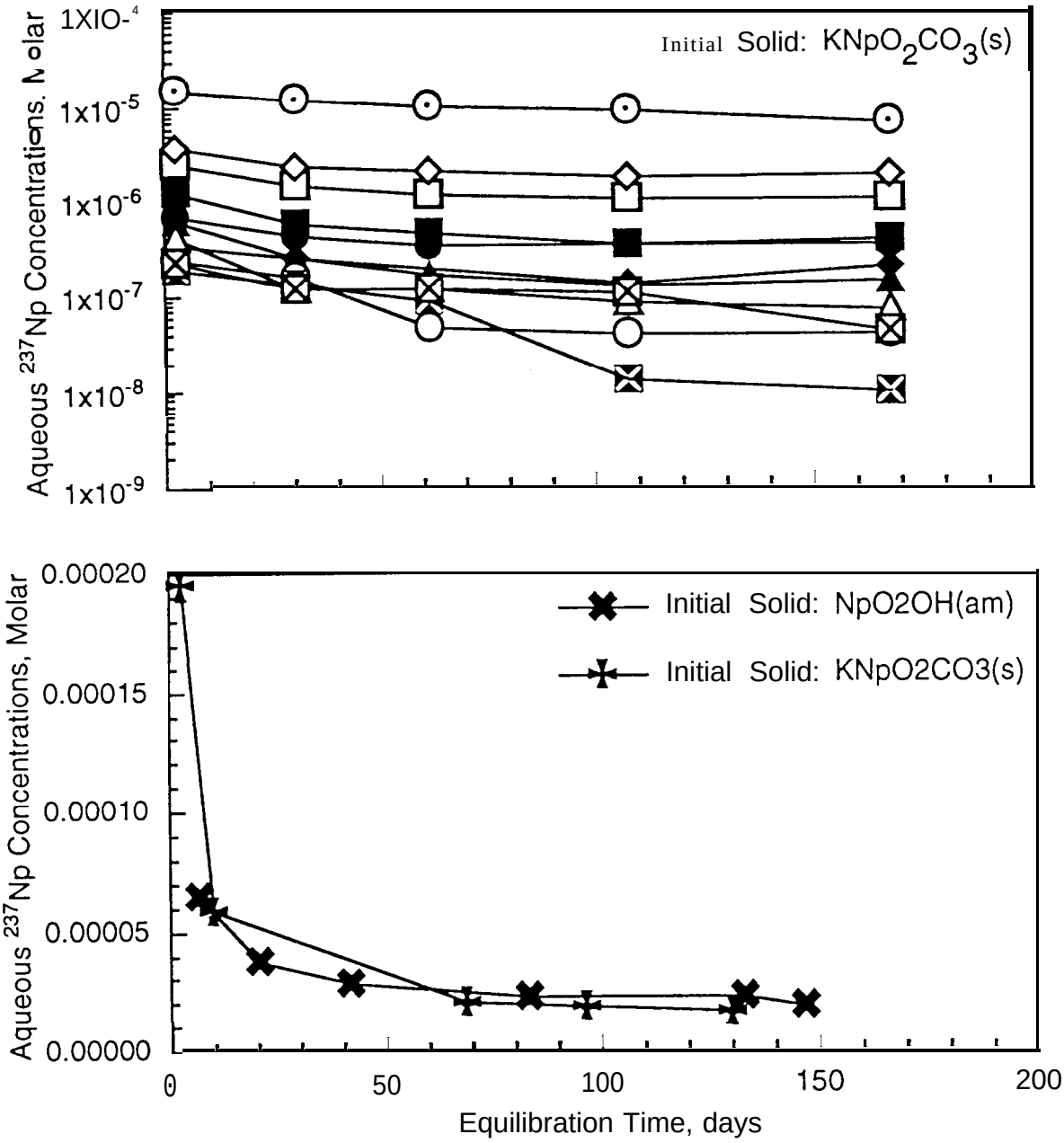

Figure 1. Approach to steady-state for the K-Cl-CO_3 series of experiments. Concentrations in (a): ■ 0.001mK_2C0_3/0.0032 mKCl, ● 0.01/0.0032, A 0.001/0.032, ● 0,01/0.032, •l 0.1/0,032, O 0.001/0.32, A 0.01/0.32, O **0.1/0.32,** ❑ **0.001/3.2,** ❑ **0.01/3.2,** ⊙ **0.1/3.2. Note** that **(b),** $1\,m_{K_2CO_3}$ + $1\,m_{KCl}$, is shown on a linear scale.

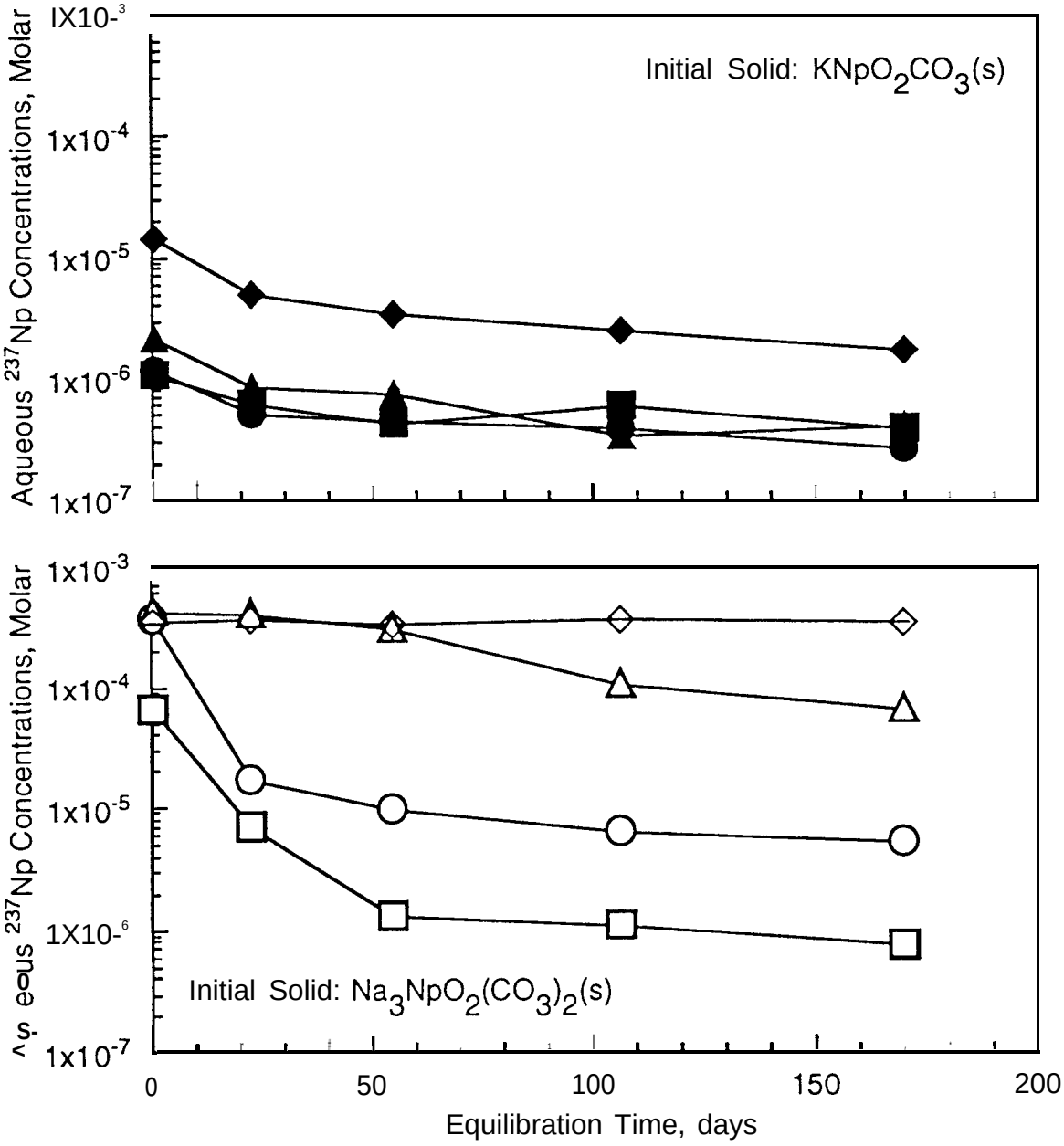

Figure 2. Approach to steady-state for the Na-K-Cl-CO_3 series of experiments, separated for clarity. Symbols represent 5m NaCl + O. 1m KCl plus : ■ 0.0004$m_{Na_2CO_3}$, ● 0.001, A 0.003, ● 0.01, ❑ 0.01, 00.05, A 0.2, 01.0.

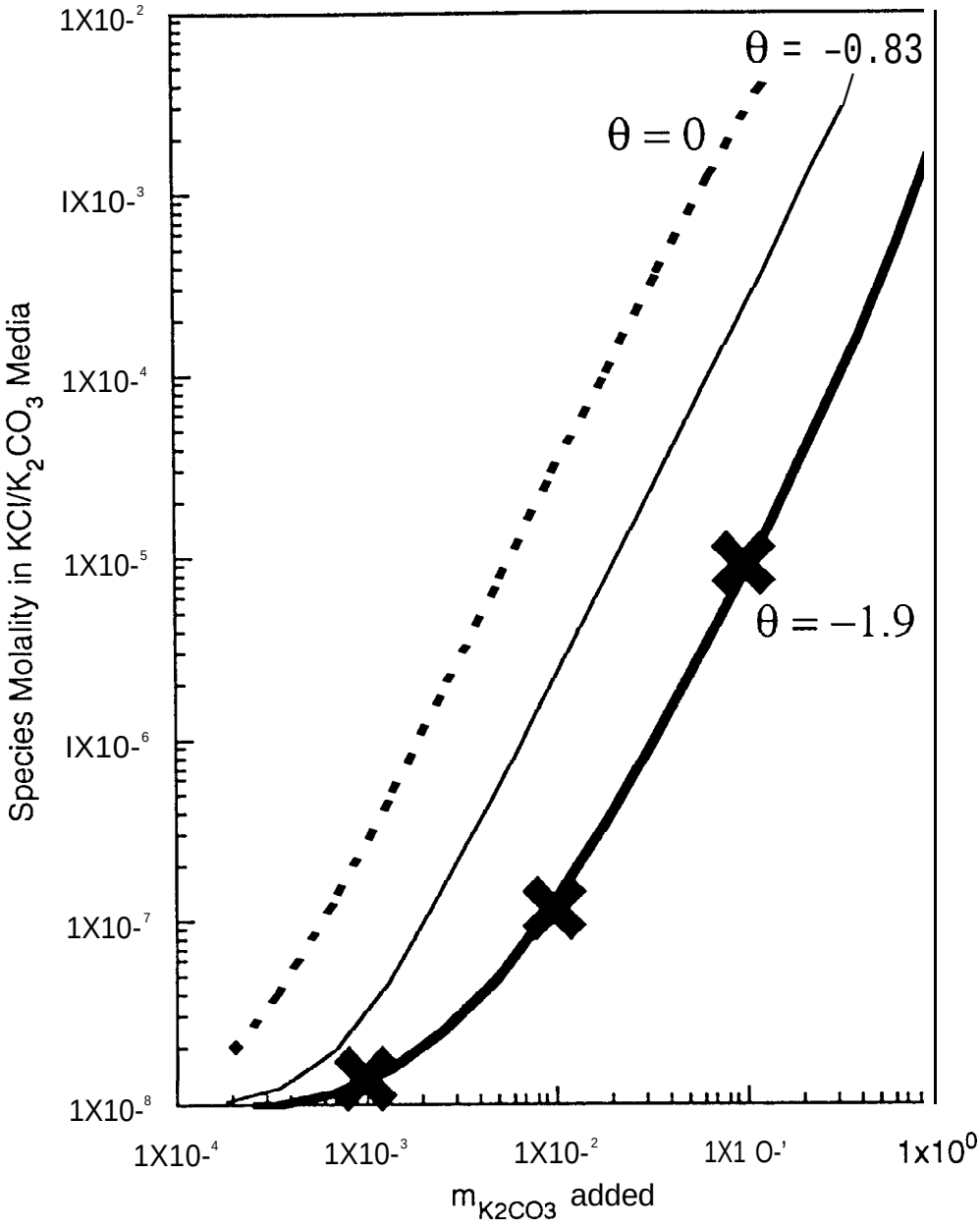

Figure 3. Comparison of volubility measurements and thermodynamic predictions of the volubility of $KNpO_2CO_3(s)$ in 3.2m KCl media as a function of K_2CO_3, for the three different values of $\theta_{CO_3\,NpO_2(CO_3)_3}$ proposed in Novak et al. (1996a).

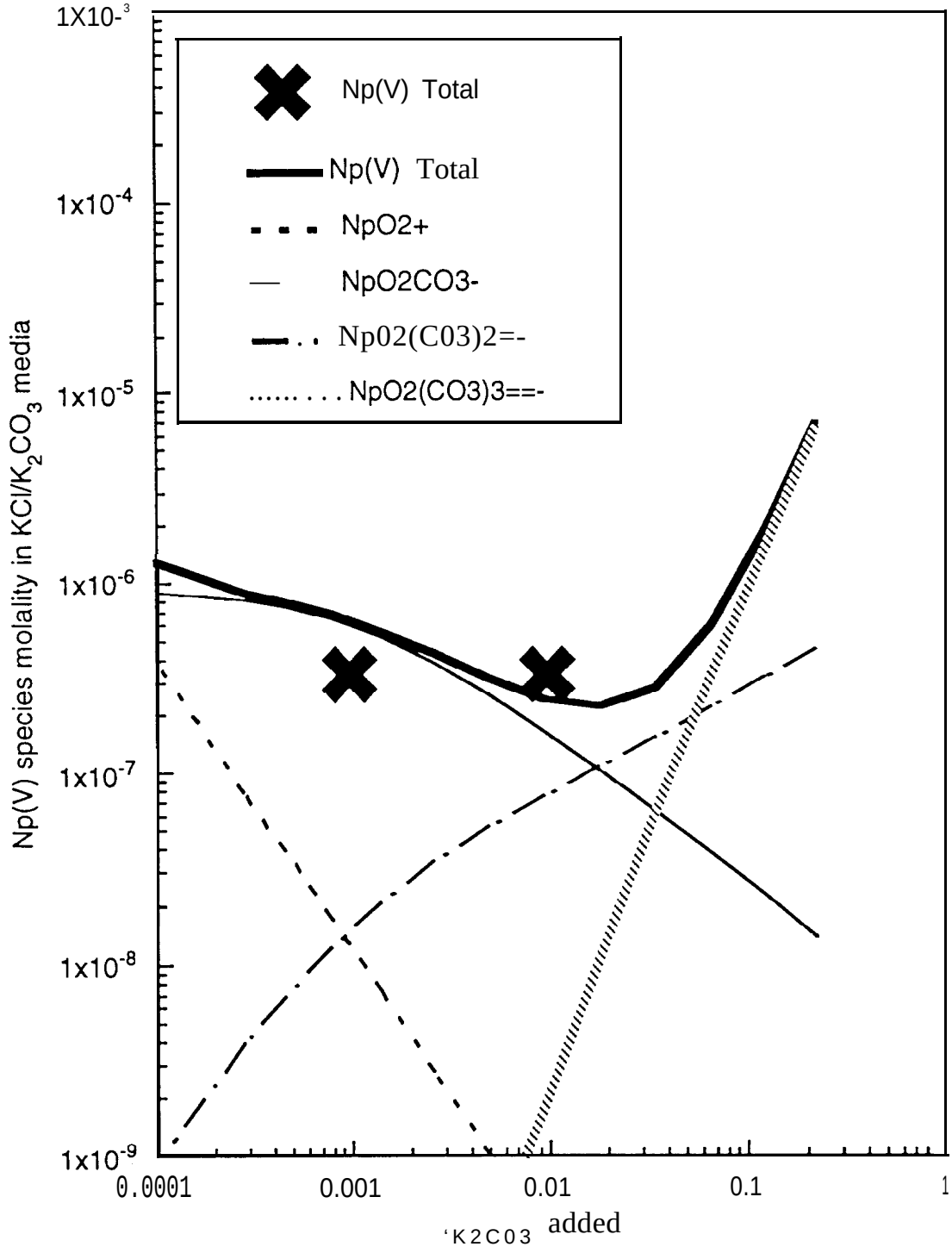

Figure 4a. Calculated volubility of $KNpO_2CO_3s$) in 0.0032m KCl media as a function of K_2C0_3, and comparison with measurements

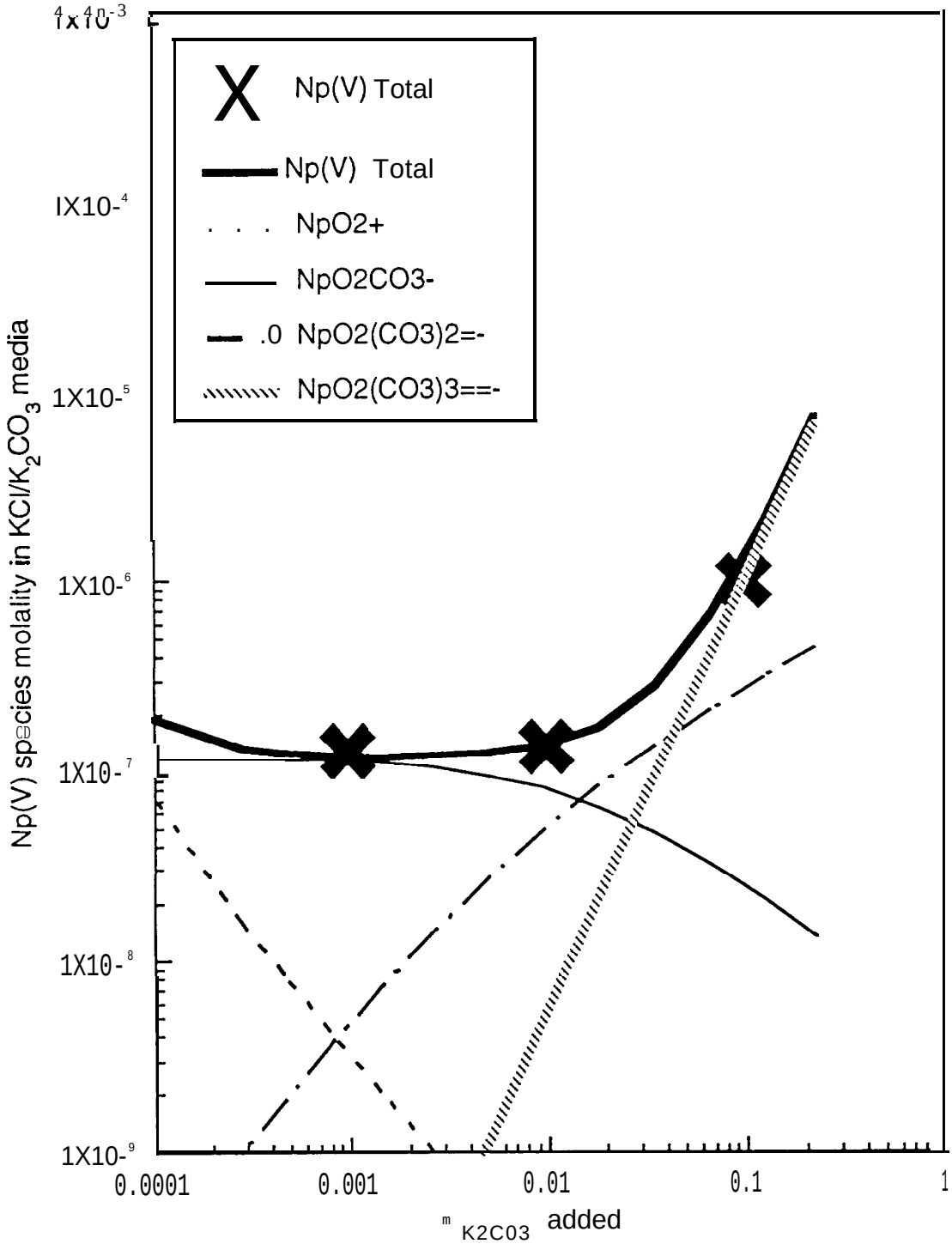

Figure 4b. Calculated volubility of $KNpO_2CO_3(s)$ in 0.032m KCl media as a function of K_2CO_3, and comparison with measurements

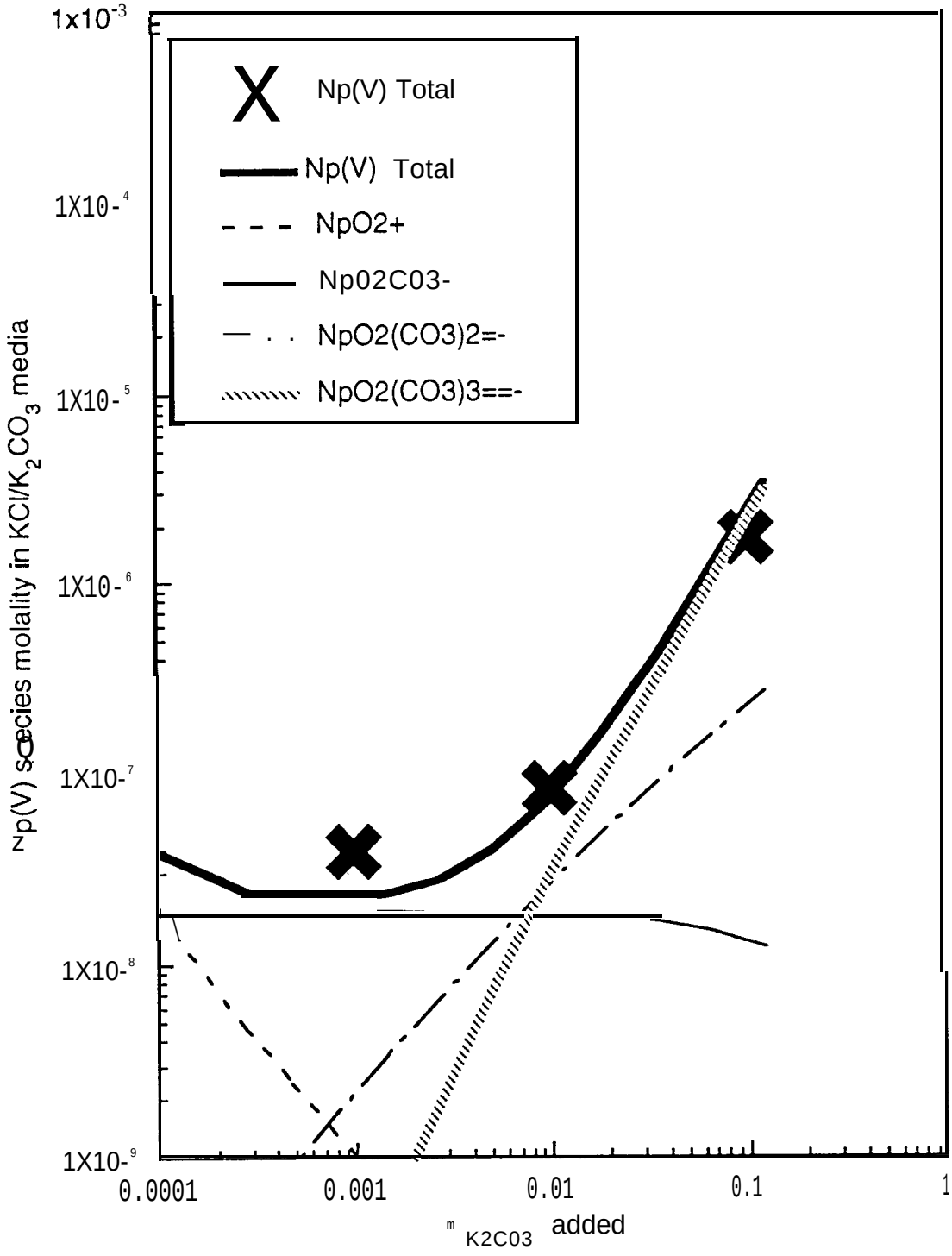

Figure 4c. Calculated volubility of $KNpO_2CO_3(s)$ in 0.32m KCl media as a function of K_2CO_3, and comparison with measurements

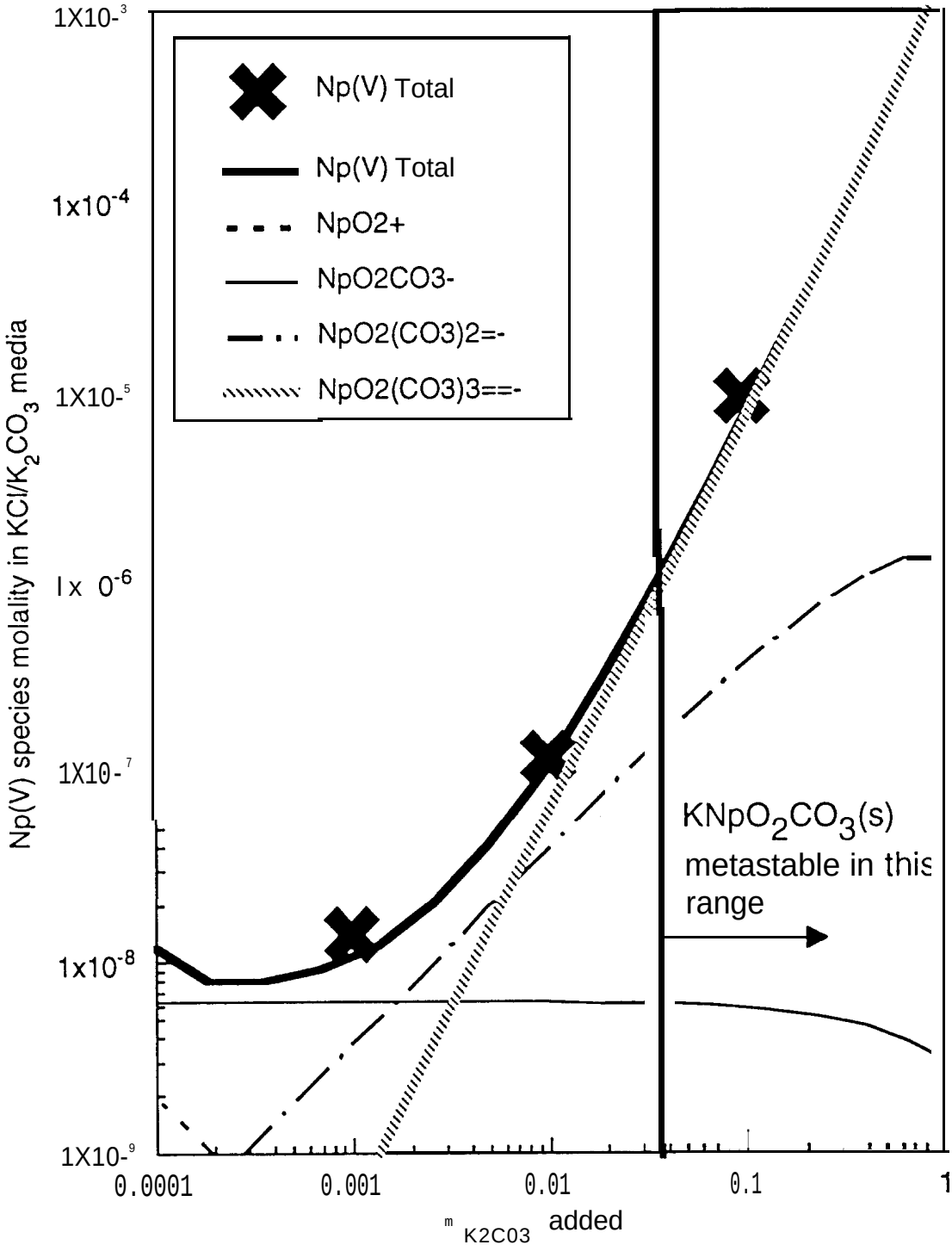

Figure 4d. Calculated volubility of $KNpO_2CO_3(s)$ in 3.2m KCl media as a function of K_2C0_3, and comparison with measurements

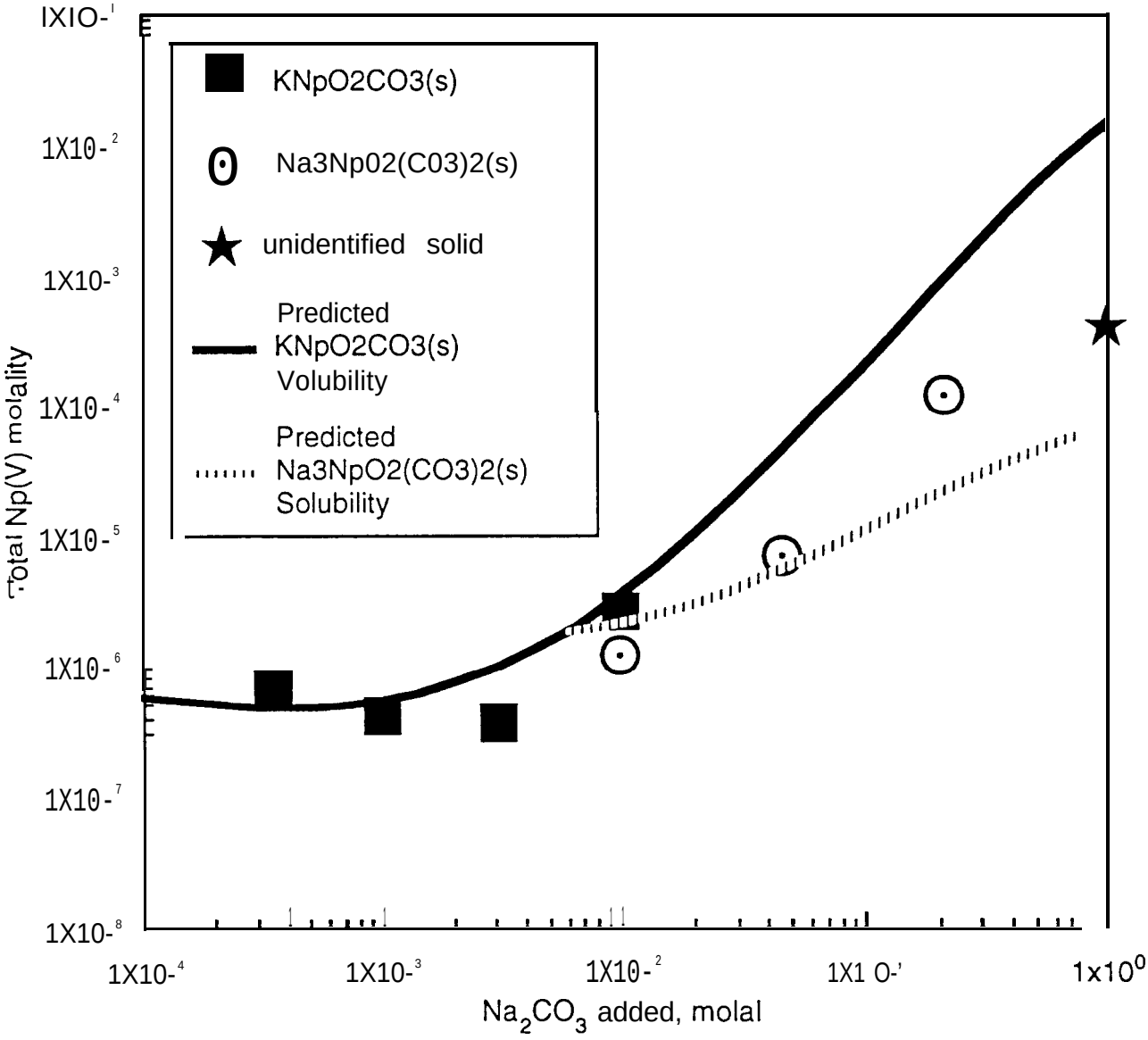

Figure 5. Comparison between experiments and predictions for the volubility of Np(V) in m_{NaCl}=5, m_{KCl}=0.1 solutions as a function of added Na_2CO_3.

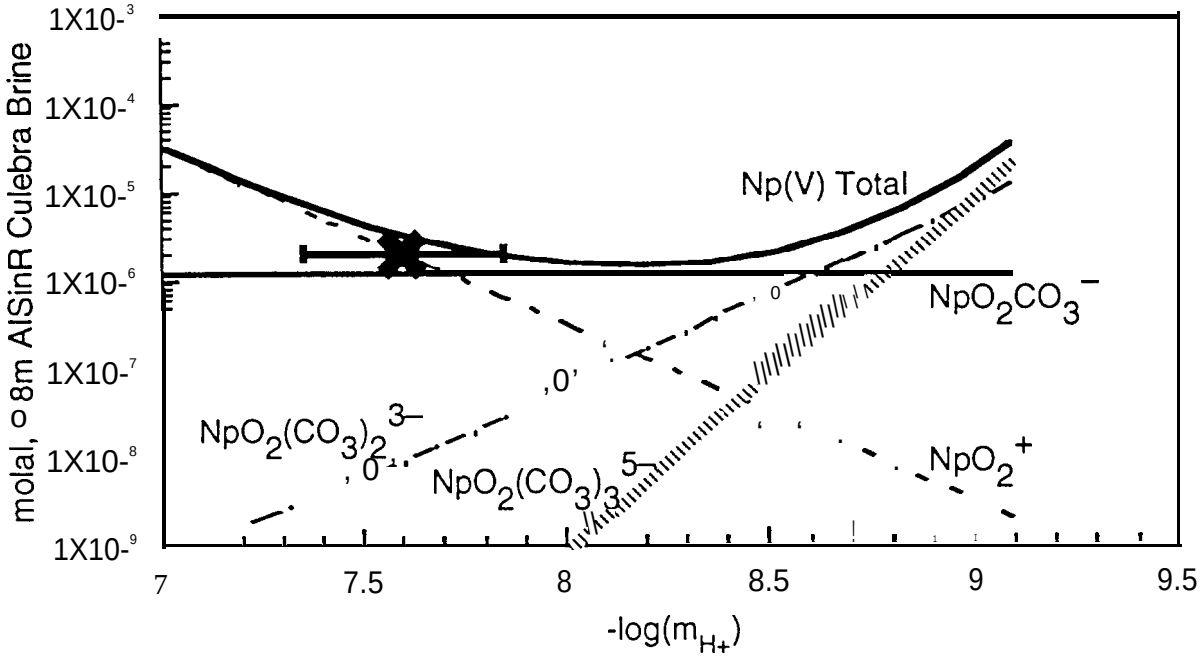

Figure 6a. Calculated $KNpO_2CO_3(s)$ volubility and Np(V) speciation in a predominantly Na-Cl brine with 0.86 molal ionic strength (see Table 5) as a function of hydrogen ion concentration, and comparison with experimental measurement.

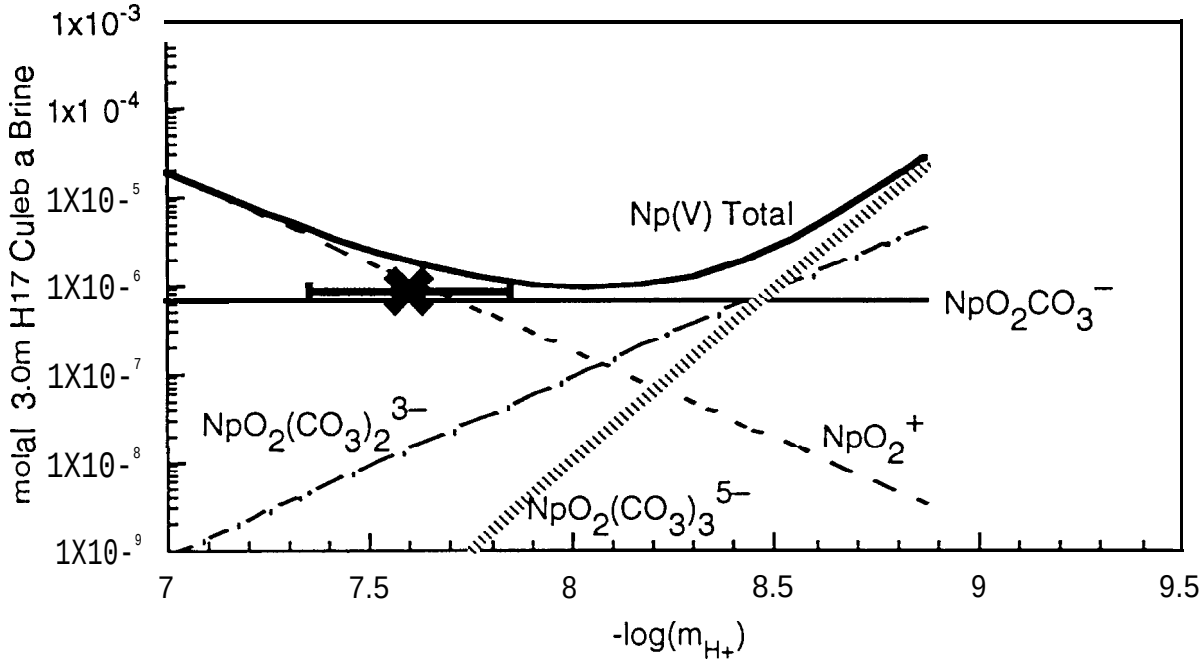

Figure 6b. Calculated $KNpO_2CO_3(s)$ volubility and Np(V) speciation in a predominantly Na-Cl brine with 3.0 molal ionic strength (see Table 5) as a function of hydrogen ion concentration, and comparison with experimental measurement.

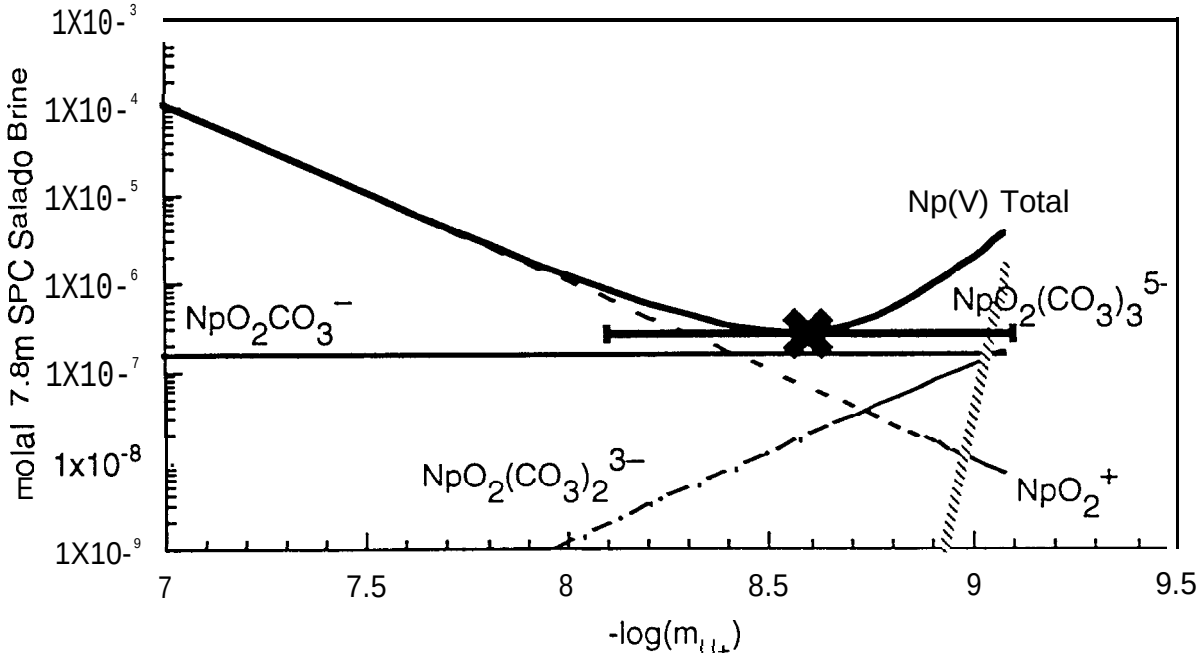

Figure 6c. Calculated $KNpO_2CO_3(s)$ volubility and $Np(V)$ speciation in a predominantly Na-Mg-K-Cl brine with 7.8 molal ionic strength (see Table 5) as a function of hydrogen ion concentration, and comparison with experimental measurement.